



Chemical Synthesis, Kinetics, and Characterization of Nano-Lead Oxide Powder

Damilola Tope OGUNDELE ^{1*} , Samsudeen Olanrewaju AZEEZ¹ ,
and Akeem Adebayo JIMOH¹ 

¹Kwara State University, Department of Chemistry and Industrial Chemistry (241103), Malete, Nigeria.

Abstract: Systematic chemical decomposition, leaching, desulfurization, reducing and precipitation of spent lead-acid batteries to extract lead in oxide form as a valuable product using organic acid, salt of the acid, and hydrogen peroxide were studied in this present work. Citric acid was found a suitable leachant to dissolve lead. With 1 M citric acid, 2 M sodium citrate, and hydrogen peroxide, 180 min reaction time, solid/liquid ratio of 100 g/L, 30 °C temperature, and 500 rpm speed, > 97% extraction of lead in citrate form was achieved. Leaching kinetics followed $1 - 3(1 - X)^{2/3} + 2(1 - X) = Kct$ ash diffusion controls dense constant-sized-spherical particles model with an activation energy of 8.3 kJ/mol. The precipitate was calcined at 400 °C to produce α - and β -PbO with a particle size of 19 nm which can be used as a raw material in the production of a new lead-acid battery.

Keywords: Leaching, kinetic study, leaching models, nanoparticle.

Submitted: May 06, 2021. **Accepted:** January 17, 2022.

Cite this: Ogundele DT, Azeez SO, Jimoh AA. Chemical Synthesis, Kinetics, and Characterization of Nano-Lead Oxide Powder. JOTCSA. 2022;9(1):227-36.

DOI: <https://doi.org/10.18596/jotcsa.928341>.

***Corresponding author.** E-mail: (oludeledamilola@gmail.com), Tel: (08034396529).

INTRODUCTION

Lead(II) oxide (PbO) nanoparticles show unique optical, electronic, magnetic, luminescent, gas sensing, ultraviolet-blocker, and catalytic properties due to their dimensions, shapes, and surrounding chemical elements (1,2). One of the diverse approaches of synthesizing PbO at nano-dimensions is simultaneous chemical leaching and precipitation of metal sulfide and metal oxides from spent lead battery paste which proved to be a profound process of reducing emission. Chemical conversion is a very simple and convenient method for particle size control at nano dimensions (3).

Nanometer dimensions of nanoparticles are reported factors that enhance the aggregation of the particles thereby influencing the size, shape, chemical, physical and biological properties. It is therefore necessary to minimize aggregation and keep the particles at desirable sizes by the use of suitable organic/inorganic reagents usually referred to as

capping agents (1). These reagents also play an important role in controlling the size and shape of nanoparticles. The metal nanoparticles contain some carboxylate groups (functional groups) which serve as capping agents in the formation of nanoparticles and bind to the metal surface of the nanoparticles. It prevents degradation and preserves the properties of the nanoparticles (16).

Wet chemical treatment of spent lead-acid battery does not involve smelting and roasting as the usual practices of recovering Pb from Spent Lead Acid Battery (SLABs) thereby, it eliminates environmental impact associated with the smelting process. The smelting process requires an enormous temperature of > 1000 °C and the emission of SO₂ gas in addition to lead fume generation (4,5). Some researchers have investigated the chemical conversion of metal components of spent batteries such as PbSO₄, PbO₂, PbO, and metallic Pb (6), but they did not carry out the kinetic study using

shrinking core model to obtain rate-controlling steps as intended by this study.

Therefore, this work aimed to synthesis PbO nanoparticles via wet chemical conversion, studied the effect of leaching temperature on leaching rate by testing all equations of shrinking core model, and obtained the activation energy for this process by Arrhenius plots.

EXPERIMENTAL

Spent lead-acid battery paste that was locally sourced, randomly homogenized, and composited

was used as a precursor for the production of PbO nanoparticles. The paste was characterized to examine the phases, morphology, and elemental composition before wet chemical conversion. The binding characteristic sites of the organic acid and its salt, and reductant used as leaching, desulfurizing, reducing, and precipitating agents are provided in Figure 1. The organic acid tested was fruit acid with polycarboxylic groups as binding sites. All the chemicals employed in the study were from Merck chemicals, AnalaR grade with high purity without further purification. Deionized water was used for all experimental works.

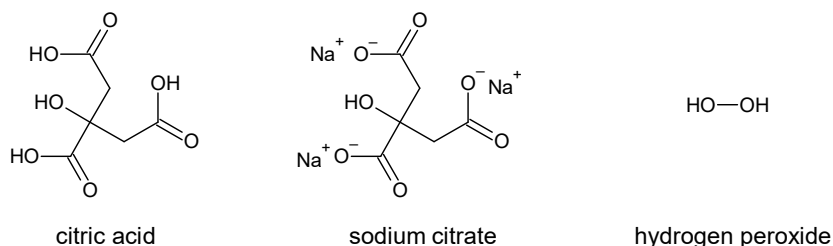


Figure 1: Structural and anchoring groups of organic acids.

The leaching of SLAB paste was done in a temperature-controlled, closed three-necked Pyrex flask glass reactor. The sample was introduced into the leachants of pre-determined pH of 3.94 for optimum leaching and precipitation in ratio 2:1:2 in different conditions determined: 1 M citric acid, 2 M sodium citrate, and 2 M hydrogen peroxide, 100 g/L (S/L), 30 °C, 500 rpm, and 3 h.

Mechanical agitation of the sample was achieved using a magnetic stirrer which was adequate to ignore the mass transfer effect during leaching. The samples were taken at an interval of time and analyzed using Atomic Absorption Spectroscopy (AAS). On completion of each experiment, the precipitate/residues were vacuum-filtered and dried at 70 °C in a temperature-controlled oven. The percentage extractions by each acid were calculated and the precipitate of best recovery was subjected to characterization. Extraction and leaching kinetics were performed to probe the mechanism of dissolution of the battery paste in organic acid. The kinetic study helps understand solid-fluid reactions of dense particles and to affirm the certainty of leaching temperature, energy consumption, and to validate the morphology obtained from the SEM spectra. All the standard equations of shrinking core models were investigated for the reaction from the data obtained during leaching experiments. This is the most widespread model elucidating on the fluid-solid reaction of dense particles. The standard equations of the model are:

$$X = K_c t \tag{Eq. 1}$$

Film diffusion control dense constant size small particles– all Geometrics

$$1 - (1 - X)^{\frac{2}{3}} = K_c t \tag{Eq. 2}$$

Film diffusion control dense shrinking spheres

$$1 - (1 - X)^{\frac{1}{2}} = K_c t \tag{Eq. 3}$$

Chemical reaction control dense constant size cylindrical particles

$$1 - (1 - X)^{\frac{1}{3}} = K_c t \tag{Eq. 4}$$

Chemical reaction control dense constant size or shrinking spheres

$$1 - 3(1 - X)^{\frac{2}{3}} + 2(1 - X) = K_c t \tag{Eq. 5}$$

Ash diffusion control dense constant size-spherical particles

where K_c = reaction rate constant (min^{-1}); t = time (min); X = fraction reacted of Pb (% extraction/100)(7).

Material Characterization

The precipitate was calcined at 400 °C pre-determined calcination temperature by Thermo Gravimetric Differential Thermal Analysis (TG-DTA) and instrumental characterizations were carried out to substantiate the lead oxide nanoparticle/ powder. X-ray diffraction patterns of powdered samples were

collected using Bruker X-ray diffractometer (XRD, D8 Discovery, US) with Cu-K α radiation and $\lambda=1.5406 \text{ \AA}$. The morphology of the samples was examined using a Field emission gun-scanning electron microscope (Model FEI 430) fitted with an energy dispersive X-ray spectrometer (FEG-SEM/EDAX) and operated at 15.0 kV after coating the sample with silver. EDX spectra were collected on SEM/EDX SDD Apollo 40 Resolution 131.44 Model FEI 430. Thermal analyses were conducted on lead citrate precursors using a platinum crucible and alumina reference recorded on HITACHI STA 7300. FTIR spectra were recorded

on a Nicolet 5700 spectrometer using the KBr pellet method.

RESULTS AND DISCUSSION

XRD Analysis of SLAB Paste

The X-ray diffraction pattern of the paste is shown in Figure 2. Chemical phases in the paste revealed PbSO₄, PbO₂, PbO, Pb₃O₂SO₄ and metallic Pb. These phases are in line with chemical phases identified by literatures except for Pb₃O₂SO₄ identified in this research (6,8).

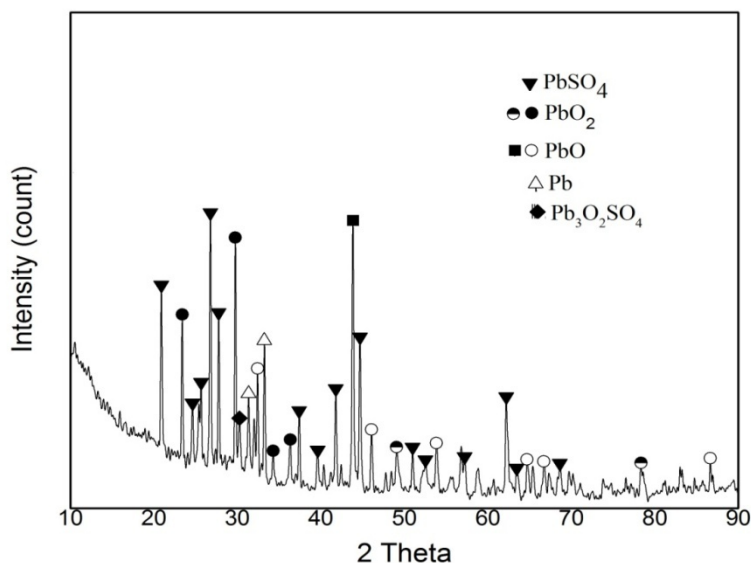


Figure 2: XRD pattern of used lead-acid battery paste.

FE-SEM, EDS Analysis of SLAB Paste

Figure 3 shows the typical morphology of the spent paste from automobile car batteries. Bulk and area scanning of the paste revealed a greater percentage of the micrograph as lead sulfate as compared to the image of PbSO₄ by (9).The energy dispersive spectra of point analysis obtained confirmed the

presence of Pb, O, S, Fe, as dominant elements in the paste and trace amount of carbon as the sample was coated on carbon tape. The percentages of Pb 63%, sulfur 11%, oxygen 18%, and iron 5% showed that the material is predominantly lead sulfate with traces of iron.

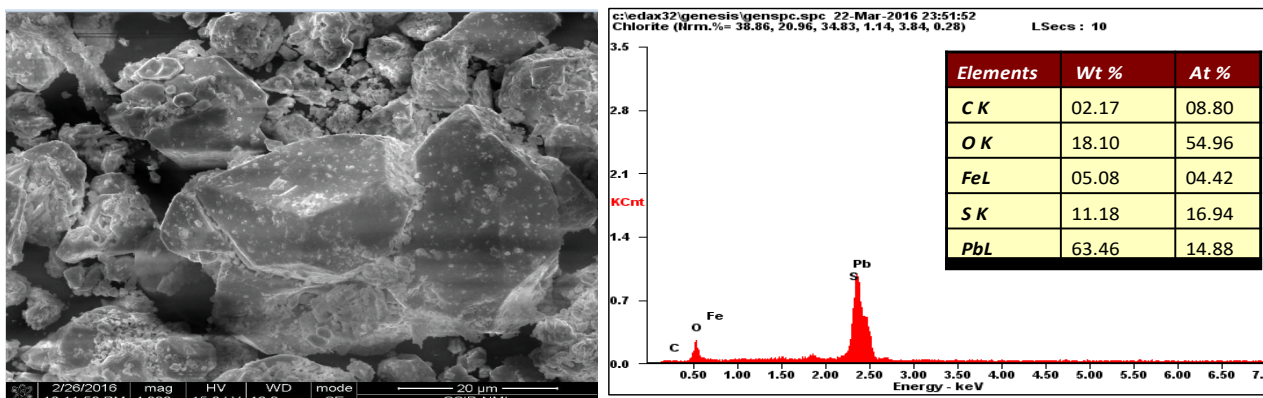


Figure 3: FE-SEM, EDS spectra of spent lead-acid battery paste.

XRD Analysis of Lead Citrate

The XRD phase of the synthesized lead citrate is shown in Figure 4. None of the phases identified in the paste were observed in the resulting precipitate indicating complete reaction between the paste and the leaching agents.

FE-SEM, EDS Analysis of Lead Citrate

The morphology of the lead citrate is revealed in Figure 5. The citrate is sheet-shaped which filtered out of the leaching solution with ease. The morphology changed from the block material to a sheet-like shape after the reaction. Energy dispersive spectra of the synthesized lead citrate

gave the percentages of elements present in the precursor as lead 81%, sulfur 1%, oxygen 7%, and carbon 9% (Figure 4) against the percentages of these elements in the paste lead 63%, sulfur 11%, iron 5%, oxygen 18%, and carbon 2% (Figure 3). Deducing from these results, sulfur in the paste has been reduced drastically from 11% to 1% which was the major process (desulfurization). It was also observed that iron was present in the paste but has been eliminated in the precipitate probably as iron sulfate. This observation affirms the purity of the lead citrate synthesized. The lead citrate was used to synthesize the desired PbO nano-sized particles.

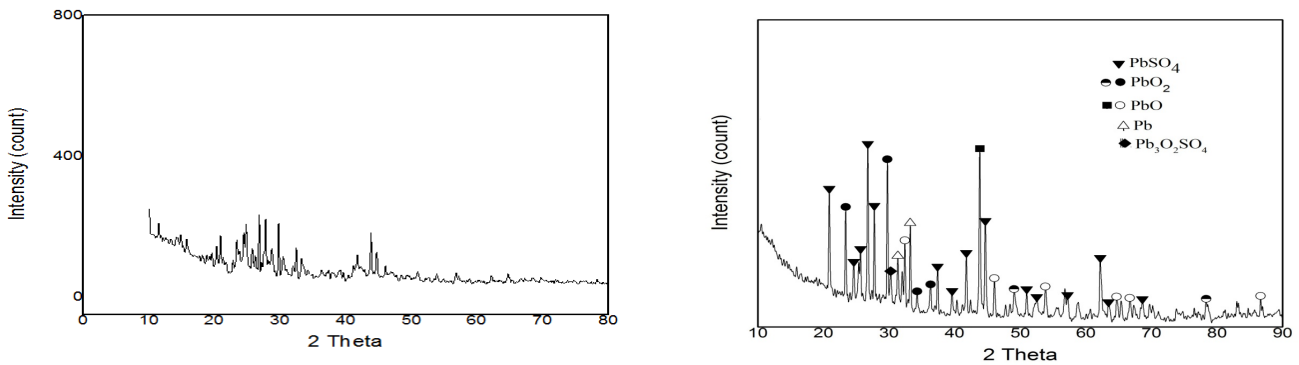


Figure 4: XRD patterns of citric acid synthesized precipitate (left) and spent paste (right).

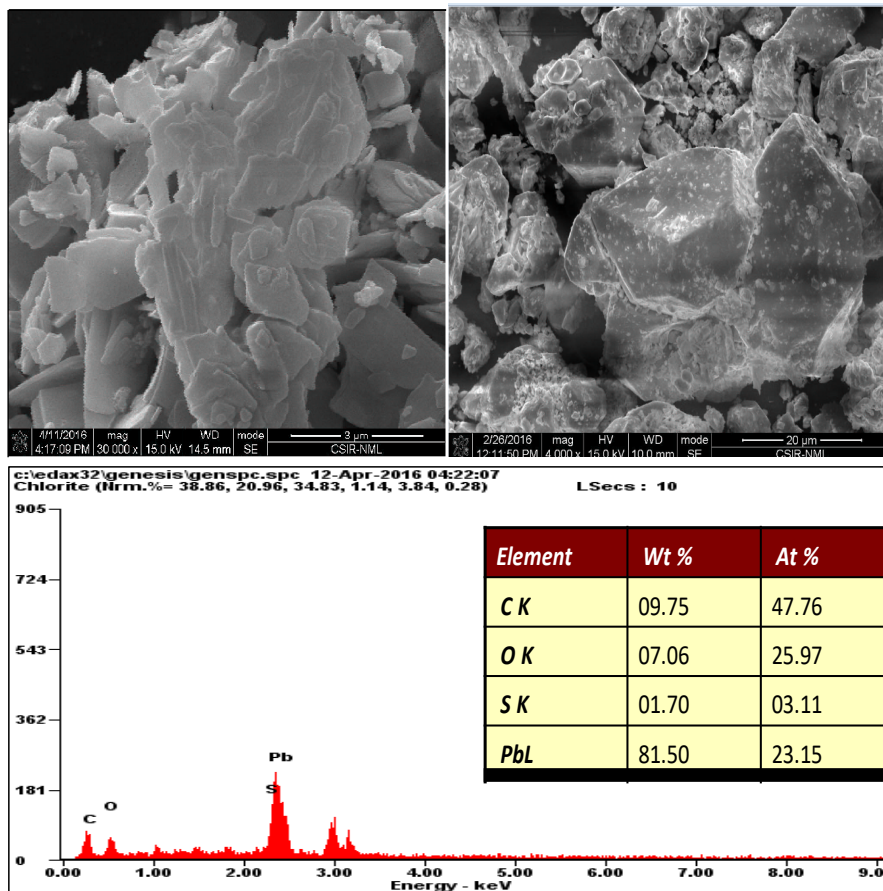


Figure 5: FE-SEM, EDS spectra of lead citrate precipitate and spent paste.

FT-IR Analysis of Lead Citrate

The FT-IR spectrum in Figure 6 was obtained to analyze the vibrations of the groups present in the lead citrate synthesized. FT-IR analysis showed strong absorption of carboxylate structure. The band 3415 cm^{-1} revealed O-H strong stretching, while 2925 cm^{-1} showed C-H stretching. Symmetric vibration of the range 1567 cm^{-1} to 1400 cm^{-1}

belonged to the carboxylate group. The weak bands of 1268 cm^{-1} to 1074 cm^{-1} are the C=O stretching which is a characteristic of citric acid. The band at 916 cm^{-1} in the fingerprint region showed C-H stretching and the band 622 cm^{-1} denotes the Pb-O-Pb bond. The strong intense peak of 1400 cm^{-1} is a result of O-H bending vibration in adsorbed water (1).

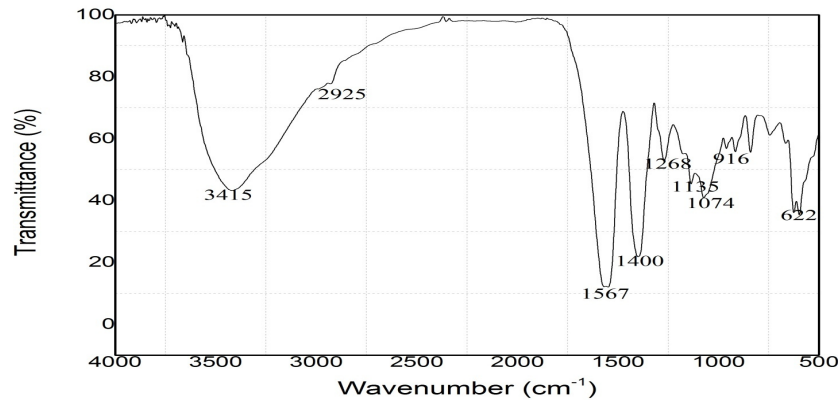


Figure 6: FT-IR spectrum of lead citrate precipitate.

XRD Analysis of Nano-PbO

The XRD pattern of the nano lead oxide powder obtained after thermal treatment of the lead citrate

matched well with the tetragonal and orthorhombic PbO of JCPDS,1986 with intense peaks as shown in Figure 7.

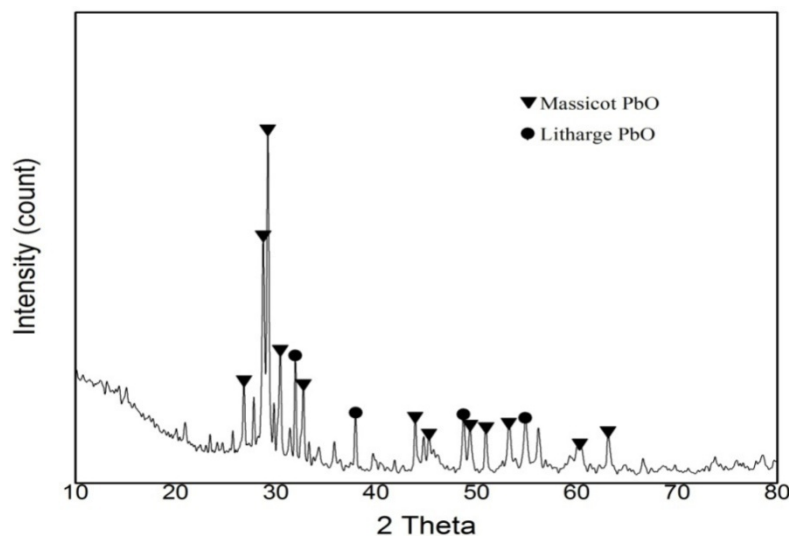


Figure 7: XRD spectra of nano-PbO.

XRD-Particle Size

An XRD analysis of the prepared sample PbO was carried out using X'pert PRO PANalytical diffractometer, Cu-K α X-rays of wavelength (λ) 1.5406 \AA . XRD pattern of Lead Oxide nanoparticle prepared is shown in Figure 7. The average size of the product was calculated using the Debye-Scherrer formula (1).

$$D = 0.9 \frac{\lambda}{\beta} \cos \theta \quad (\text{Eq. 6})$$

where D is the mean particle size; λ is the wavelength of CuK α - 1.5406 \AA ; β is the full width at half maximum (FWHM); and θ is Bragg's diffraction angle. The particle size calculated by the above formula was 19 nm . This result is in line with (17).

FE-SEM and EDS of Nano-PbO

The SEM and EDS spectra of nano-PbO obtained show a high agglomeration of the particles. The nano-PbO is spherical. The SEM morphology of the products as shown in Figure 8 revealed the particle size of the products at a range of 19 nm (16). This

is similar to what was reported in (13). The morphology of the lead citrate was observed to have changed from a sheet-like structure with the calcination temperature. The particles were agglomerated at the 400 °C pre-determined temperature from our previous publication. EDS spectra showed significant peaks identified to be

characteristic peaks of Pb and O proving that the products were mainly lead oxide.

The color of the products changed from the dark SLAB paste to whitish color of the lead citrate before calcination to yellow products of nano lead oxide Figure. 9(10)

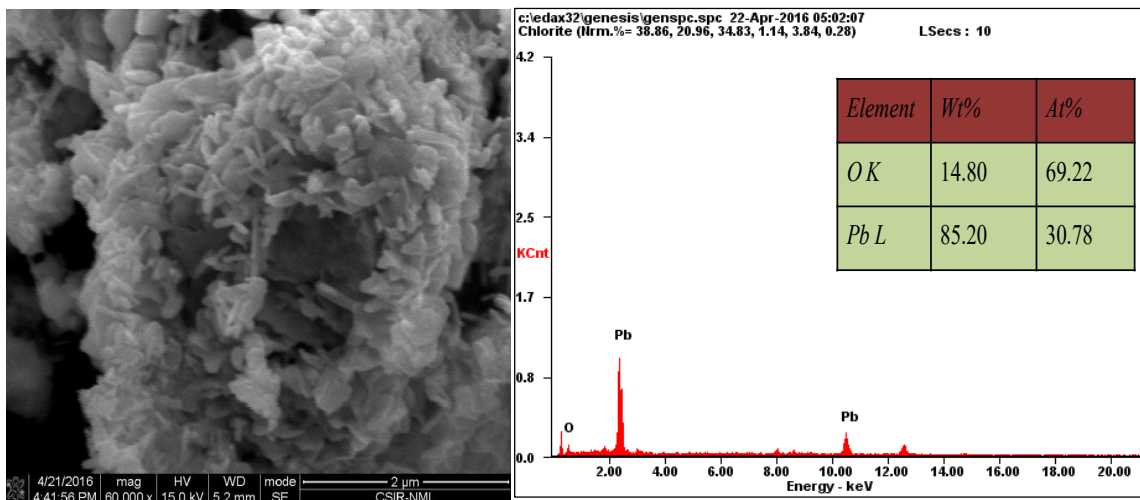


Figure 8: SEM, EDS images of nano PbO.

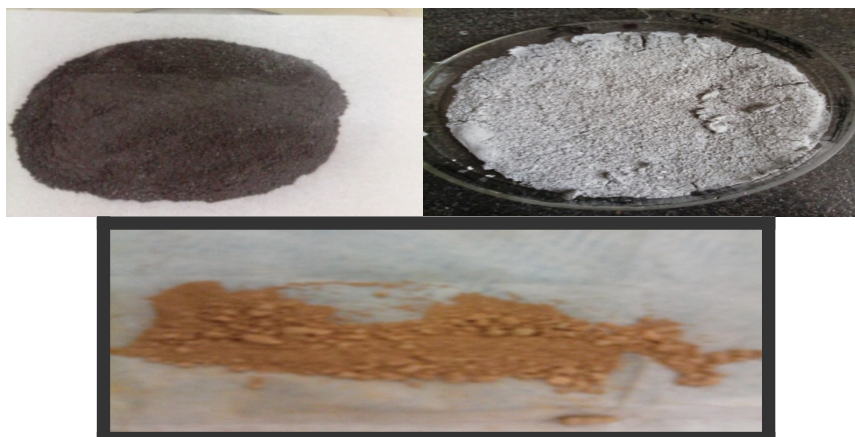


Figure 9: Color changes of the samples.

Specific Surface Area (SSA)

This is one of the properties of solids which is the total surface area of a material per unit mass. It is scientifically derived and is applied to ascertain the type and properties of materials. It has several applications in adsorption, heterogeneous catalysis, and reaction on surfaces. It can be determined by the formula:

$$SSA = \frac{SA_{part}}{V_{part} \times \text{Density}} \quad (\text{Eq. 7})$$

where SSA is the specific surface area; SA part is the surface area of the particle; V part is particle volume; and Density is the theoretical density of lead oxide. SSA can also be calculated using Equation 8:

$$S = 6 \times \frac{10^3}{D \rho} \quad (\text{Eq. 8})$$

where S is the specific surface area; D is the mean particle size; ρ is the density of lead oxide. Mathematically, both relations give the same value. SSA calculated by the formula was 33 m²/g (11,17).

Crystallinity Index (I_{cry})

The crystallinity of a solid defines the degree of structural order in the solid. It is determined by comparing particle size measured from XRD data with particle size from SEM/TEM measurement. It can be calculated using the relation:

$$I_{cry} = \frac{D_p}{D} \quad (\text{Eq. 9})$$

where D_p is the particle size from SEM/TEM; and D is the particle size from the Scherrer formula (11).

If the I_{cry} value is close to 1, it is assumed the particle size is monocrystalline; and where it is greater than or much larger, it is assumed to be polycrystalline. The calculated crystallinity index was 3, which implied that the product was polycrystalline (15).

Leaching Kinetic Studies

The leaching kinetics studies of the paste were done by experimenting at different reaction times and different acid concentrations with pulp density (S/L) ratio of 100 g/L. The result is presented in Figure 10; an increase in acid concentrations increased the lead in solution at a varied time. All standard equations of shrinking core models were analyzed for reaction kinetics of lead dissolution.

Examination of the experimental results in all the models using the above equations, the kinetics followed Ash diffusion control model, i.e $1-3(1-X)^{2/3}+2(1-X) = K_c t$ as exemplified in Figure 10 and Table 1 for 1 M and 3 M citric acid concentration

while at 2 M concentration, chemical reaction control model was best fitted. The ash diffusion model was affirmed by the SEM/EDX studies. The spongy structure of the leached residue indicated that elemental Pb was deposited during the early period of leaching. The deposited Pb acted as a permeable layer permitting ash diffusion-control reaction kinetics, the SEM image is shown in Figure 11. The model fitted at 2M citric acid with $1-(1-X)^{1/2} = K_c t$ chemical reaction control dense cylindrical particles. This is depicted in the SEM photograph in Figure 10 which confirmed the model of the reaction. The equations were selected based on the highest values of R^2 the regression coefficient in each study Figure 12. The Activation energy of the ash diffusion control model was calculated using Arrhenius' equation $K_c=Ae^{-E_a/RT}$ to be 8.3 kJ/mol and the chemical control model was 33.3 kJ/mol. Michael (12) reported that aqueous diffusion control reactions often have low activation energies of less than 15,000 J/mol. and chemical control has larger activation energies. The reactions in this study are not strongly influenced by temperature as room temperature was found suitable for the experiments which confirmed kinetic reaction processes. Lead(II) oxides (α,β) at a nano dimension of 19 nm and a specific surface area of 33 m²/g polycrystalline were produced.

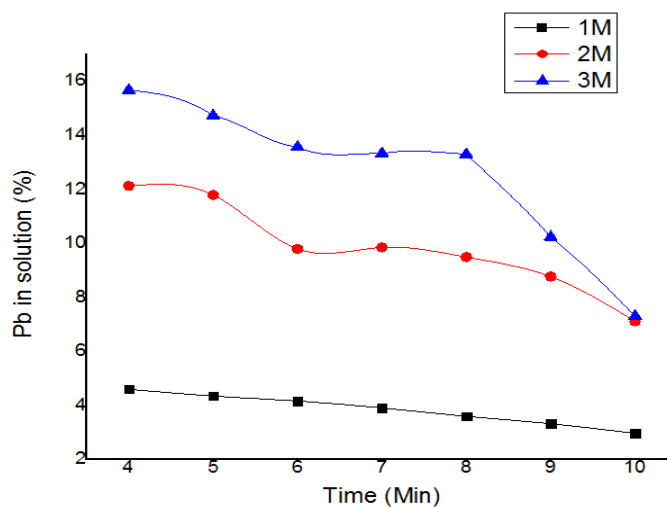


Figure 10: Kinetics of Pb leaching at 100 g/L with citric acid.

Table 1: Regression Coefficient Values for different shrinking core models for the kinetics of leaching of lead-acid battery paste.

S/N	Citric Acid conc. (M)	X	$1-(1-X)^{2/3}$	$1-(1-X)^{1/2}$	$1-(1-X)^{1/3}$	$1-3(1-X)^{2/3}+2(1-X)$	Model selected
A	1		0.9927	0.9928	0.9929	0.9979	$1-3(1-X)^{2/3}+2(1-X)$
B	2		0.9207	0.9209	0.921	0.9199	$1-(1-X)^{1/2}$
C	3		0.8409	0.8533	0.8546	0.8983	$1-3(1-X)^{2/3}+2(1-X)$

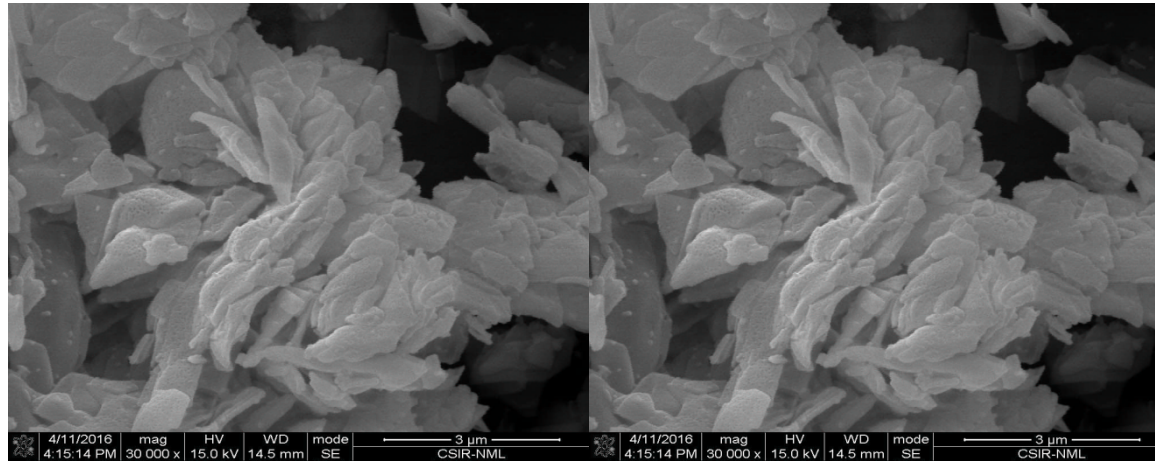


Figure 11: SEM images of leached residue for kinetics studies.

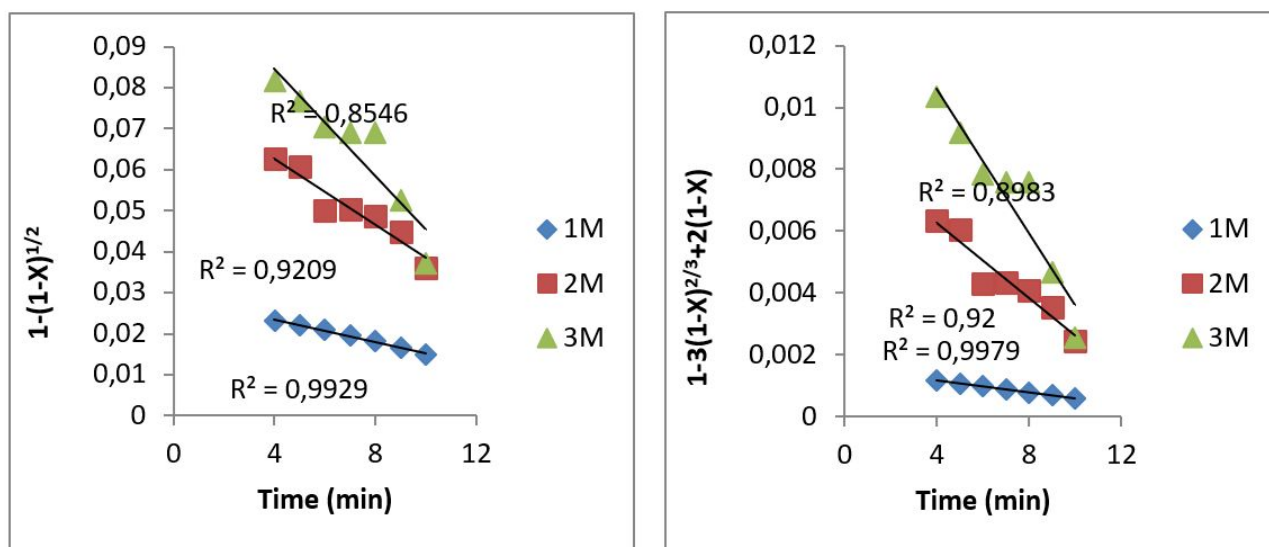


Figure 12: Fittings of lead conversion into equations of shrinking core model for lead-acid battery paste. Chemical reaction control dense constant size cylindrical particles (left), Ash diffusion control dense constant size- spherical particles (right).

CONCLUSION

Wet chemical synthesis of nano-PbO from spent SLABs via citric acid system was demonstrated in this study. Characterization of the nano powder revealed spherically shaped PbO at nano dimension. Citric acid showed good adhesive properties to the Pb component of the spent paste. A combination of pure α - β PbO was synthesized as final product without impurities. The product is suitable as raw material in the fabrication of new lead acid battery as the combination is most desired industrially. The reaction kinetics of the paste follows ash diffusion control model leaching with citric acid system. The activation energies of the overall reactions are 8.3 kJ/mol and 33.3 kJ/mol for 1 & 3 M acid system ash diffusion and 2 M chemical control acid system respectively.

ACKNOWLEDGMENTS

The researchers express their profound gratitude to *i-PSG* of CSIR- National Metallurgical Laboratory Jamshedpur, India for providing analytical facilities to fulfilling the experimental data collection.

AUTHORS' CONTRIBUTIONS

The authors designed and carried out the experiment and analyzed the experimental data. All the authors worked on characterization analysis and the drafting of the manuscript. All authors read and approved the final manuscript.

FUNDING

This work was supported by the Tertiary Education Trust fund of the Federal Republic of Nigeria and the Centre for Science & Technology of the Non-aligned and Other Developing Countries (NAM S& T) for the RTF-DCS fellowship (NAM - 05/74/2015).

COMPETING INTERESTS

The authors declare that there were no competing interests.

REFERENCES

1. Arulmozhi KT, Mythili N. Studies on the chemical synthesis and characterization of lead oxide nanoparticles with different organic capping agents. *AIP Advances*. 2013 Dec;3(12):122122. <DOI>.
2. Alagar M, Theivasant T, Raja AK. Chemical Synthesis of Nano-sized Particles of Lead Oxide and their Characterization Studies. *J of Applied Sciences*. 2012 Feb 1;12(4):398-401. <DOI>.
3. Liu N, Senthil RA, Zhang X, Pan J, Sun Y, Liu X. A green and cost-effective process for recovery of high purity α -PbO from spent lead acid batteries. *Journal of Cleaner Production*. 2020 Sep;267:122107. <DOI>.
4. Sonmez MS, Kumar RV. Leaching of waste battery paste components. Part 1: Lead citrate synthesis from PbO and PbO₂. *Hydrometallurgy*. 2009 Jan;95(1-2):53-60. <DOI>.
5. Sonmez MS, Kumar RV. Leaching of waste battery paste components. Part 2: Leaching and desulphurisation of PbSO₄ by citric acid and sodium citrate solution. *Hydrometallurgy*. 2009 Jan;95(1-2):82-6. <DOI>.
6. Li L, Zhu X, Yang D, Gao L, Liu J, Kumar RV, et al.

Preparation and characterization of nano-structured lead oxide from spent lead acid battery paste. *Journal of Hazardous Materials*. 2012 Feb;203-204:274-82. [<DOI>](#).

7. Li X, Xing P, Du X, Gao S, Chen C. Influencing factors and kinetics analysis on the leaching of iron from boron carbide waste-scrap with ultrasound-assisted method. *Ultrasonics Sonochemistry*. 2017 Sep;38:84-91. [<DOI>](#).

8. Zhu X, Li L, Sun X, Yang D, Gao L, Liu J, et al. Preparation of basic lead oxide from spent lead acid battery paste via chemical conversion. *Hydrometallurgy*. 2012 Apr;117-118:24-31. [<DOI>](#).

9. Sajadi SAA. A Comparative Investigation of Lead Sulfate and Lead Oxide Sulfate Study of Morphology and Thermal Decomposition. *AJAC*. 2011;02(02):206-11. [<DOI>](#).

10. Mahmoudabad MK, Kashani-Motlagh MM. Synthesis and characterization of PbO nanostructure and NiO doped with PbO through combustion of citrate/nitrate gel. *Int J Phys Sci*. 2011;6(24):5720-5. [<DOI>](#).

11. Nowsath Rifaya M, Theivasanthi T, Alagar M. Chemical Capping Synthesis of Nickel Oxide Nanoparticles and their Characterizations Studies. *NN*. 2012 Dec 1;2(5):134-8. [<DOI>](#).

12. Free M. *Hydrometallurgy: fundamentals and*

applications [Internet]. 2013 [cited 2022 Jan 17]. Available from: <http://site.ebrary.com/id/1075340018>. ISBN: 978-1-118-23077-0.

13. Jenkins R, Fawcett TG, Smith DK, Visser JW, Morris MC, Frevel LK. JCPDS — International Centre for Diffraction Data Sample Preparation Methods in X-Ray Powder Diffraction. *Powder Diffr*. 1986 Jun;1(2):51-63. [<DOI>](#).

14. Bratovcic A. Synthesis, Characterization, Applications, and Toxicity of Lead Oxide Nanoparticles. In: Chooto P, editor. *Lead Chemistry* [Internet]. IntechOpen; 2020 [cited 2022 Jan 17]. ISBN: 978-1-83962-568-8. [<URL>](#).

15. Spek AL. Structure validation in chemical crystallography. *Acta Crystallogr D Biol Crystallogr*. 2009 Feb 1;65(2):148-55. [<DOI>](#).

16. Fard MJS, Hayati P, Naraghi HS, Tabeie SA. Synthesis and characterization of a new nano lead(II) 0-D coordination supramolecular compound: A precursor to produce pure phase nano-sized lead(II) oxide. *Ultrasonics Sonochemistry*. 2017 Nov;39:129-36. [<DOI>](#).

17. Anonymous. *Lead Oxide Nanoparticles / Nanopowder* [Internet]. *Lead Oxide Nanoparticles / Nanopowder*. 2022. [<URL>](#).